Tamaki, K., Suyehiro, K., Allan, J., McWilliams, M., et al., 1992
Proceedings of the Ocean Drilling Program, Scientific Results, Vol. 127/128, Pt. 2

53. LOW-PRESSURE MELTING RELATIONS OF A BASALT FROM HOLE 797C IN THE YAMATO BASIN OF THE JAPAN SEA[1]

P. Thy[2]

ABSTRACT

One-atmosphere melting experiments, controlled to approximately the fayalite-magnetite-quartz oxygen buffer, performed on a basalt from Hole 797C crystallized olivine and plagioclase nearly simultaneously from about 1235°C and augite from about 1175°C. The liquid compositions indicate systematic trends of increasing FeO and TiO_2 and decreasing Al_2O_3 with decreasing MgO. Experimental olivine compositions vary from Fo90 to Fo78, plagioclase from An79 to An67, and augite from En49 to En46. The K_D value for the Fe^{2+} and Mg distribution between olivine and liquid is 0.31. The K_D value for the distribution of Fe^{total} and Mg between augite and liquid averages 0.24. These K_D values suggest experimental equilibrium. The K_D values for Na and Ca distribution between plagioclase and liquid range between 0.55 and 0.99 and are dependent on crystallization temperature. Projected on pseudoternary basaltic phase diagrams, the liquid line of descent moves toward increasing quartz normative compositions, revealing a typical tholeiitic crystallization trend with marked Fe and Ti enrichments. Such enrichments are a reflection of the dominance of plagioclase in the crystallizing assemblage. The experimental results can explain the marked Fe- and Ti-enrichment trends observed for the sills of the lower part of Hole 797C, but have no direct bearing on the origin of the relatively evolved high-Al basalts of Hole 794C.

INTRODUCTION

Basement rocks composed of thick basaltic sill complexes intruded into soft sediments were drilled at two sites during Ocean Drilling Program Legs 127 and 128 in the Yamato Basin of the Japan Sea. The geochemical and petrogenetic implications of these sill complexes have important bearings on tectonic models for the opening and evolution of backarc spreading in the Japan Sea. At Site 794 in the Yamato Basin, relatively primitive basaltic to evolved high-Al basaltic sills were drilled (Tamaki et al., 1990). At Site 797, also in the Yamato Basin, a sill complex composed of an upper suite of basaltic sills and a lower suite of Ti-enriched ferrobasaltic sills were drilled. Accompanying chapters discuss the groundmass mineralogy and the rock chemistry of the Japan Sea basalts (Thy, this volume). The presence of two major suites of relatively evolved basaltic rocks (high-Al basalts and ferrobasalts) suggests complex petrogenetic and tectonic regimes during the opening of the Japan Sea. The presence of ferrobasalts suggests low pressure, tholeiitic fractionation trends, while high-Al basalts point toward high pressure, calc-alkalic fractionation trends (Grove and Baker, 1984).

To evaluate these possible petrogenetic models, one-atmosphere melting experiments were conducted on a relatively primitive sample from the upper suite of Hole 797C. The selected sample (127-797C-12R-2, 74–79 cm; Table 1) was taken from the center of what appears to be a massive sill and was relatively unaffected by secondary alteration and hydration. This sill contains granular groundmass olivine (Fo_{87-89}) and subophitic to granular plagioclase (An_{72-78}). A few plagioclase phenocrysts (An_{78}) are present in the sample. Augite is the third phase to have crystallized (Mg/(Mg + Fe) = 0.65–0.72) and occurs as skeletal grains growing on the plagioclase. Titanomagnetite appears after augite crystallization as a fine-grained skeletal phase growing on the augite. This chapter presents the experimental results and briefly addresses the implications. A subsequent chapter discusses in more details the implications of the experimental results for the evolution of the basalts drilled during Legs 127 and 128 (Thy, this volume).

EXPERIMENTAL PROCEDURES

All experiments were performed at atmospheric pressure in a vertical quench furnace (Williams and Mullins, 1981) following procedures described by Lofgren (1983). Oxygen fugacity was controlled by a constant CO_2 and CO gas mixture calibrated at about 1100°C to the fayalite-magnetite-quartz (FMQ) buffer and measured by a ZrO_2 ceramic oxygen electrolyte cell. Temperature was monitored by Pt/90Pt-10Rh thermocouples calibrated to the melting point of gold and diopside, according to the 1968 International Practical Temperature Scale. About 100 mg of rock powder was pressed into pellets and sintered to 0.008-in. Pt-wire loops (Donaldson et al., 1975) and inserted into the furnace directly at the experimental temperature. The experiments lasted from 24 hr near the liquidus to about 190 hr closer to the solidus (Table 2).

Phases were analyzed with the electron microprobe using an acceleration voltage of 15 kV and a beam current of approximately 25 nA. A scanning-mode counting over an area of approximately 200 μm^2 was used for analyzing glasses to minimize the loss of Na. Counting times were 30–70 s, except for Na, which in glasses was counted first and for 10 s. An evaluation of the accuracy and precision of glass analyses using the VG-2 glass standard (Jarosewich et al., 1979) is given in Table 3.

EXPERIMENTAL RESULTS

Details of the 1 atm runs are presented in Table 2 and are summarized in Figure 1. The selected sample crystallized olivine and plagioclase almost simultaneously from 1235°±6°C and augite at 1175°±5°C. The phase proportions and the amounts of liquid remaining were estimated by least squares, linear regression calculations using the analytical data presented in Tables 4–7. The calculations weighted all oxides by 1.0, except SiO_2 and Al_2O_3, which were weighted 0.4 and 0.5, respectively. The result of these calculations (Table 2) reflects a systematic variation in the liquid remaining, temperature, phase proportions (Fig. 1), and Mg/(Mg + Fe^{2+}) of the liquid (Fig. 2). The liquid remaining reaches 27 wt%, below which the liquid cannot be analyzed with the broad-beam technique because of the restricted size of the analyzable areas.

For each experimental charge, 4–6 points were analyzed for each phase, and average analyses are given in Tables 4–7. Attempts were made to analyze only equilibrium phases. The standard deviations of replicate analyses of glass range between 0.12 and 0.25 for SiO_2, 0.02

[1] Tamaki, K., Suyehiro, K., Allan, J., McWilliams, M., et al., 1992. *Proc. ODP, Sci. Results*, 127/128, Pt. 2: College Station, TX (Ocean Drilling Program).
[2] NASA, Johnson Space Center, SN2, Houston, TX 77058, U.S.A. (Present address: Department of Geology, University of Botswana, Private Bag 0022, Gaborone, Botswana).

Table 1. Chemical composition of starting material (127-797C-12R-2, 74–79 cm).

	1	2
SiO_2	49.31	49.03
TiO_2	1.12	1.06
Al_2O_3	17.96	17.98
FeO*	7.56	7.82
MnO	0.16	0.15
MgO	9.59	9.79
CaO	11.30	11.02
Na_2O	2.82	3.03
K_2O	0.07	0.11
P_2O_5	0.11	
Total	100.00	100.00
Mg/(Mg + Fe)	0.693	0.691

Analyses are normalized to 100%. FeO* - Total iron calculated as FeO. Mg/(Mg + Fe) calculated with all Fe as Fe^{2+}.
1. Shipboard analysis as modified by S. Yamashita (pers. comm., 1991).
2. XRF analysis by S. Grundvig, University of Aarhus.

Table 2. Experimental conditions and results.

Run no.	Temperature (°C)	Time (hr)	Run products[a]	Phase proportions[b]				Losses (wt%)	
				gl	ol	pl	aug	FeO	Na_2O
237	1240	42	gl						
215	1231	24	gl, ol, pl	93	3	4		0.01	0.01
216	1221	24	gl, ol, pl	87	5	8		0.22	0.00
217	1212	68	gl, ol, pl	81	5	14		0.50	0.00
218	1200	70	gl, ol, pl	72	8	20		0.21	0.00
219	1190	72	gl, ol, pl	69	9	22		0.38	0.00
220	1180	119	gl, ol, pl	59	11	30		0.19	0.00
221	1171	117	gl, ol, pl, aug	55	13	32	0	0.02	0.08
222	1160	186	gl, ol, pl, aug	37	15	44	5	0.00	0.08
223	1149	189	gl, ol, pl, aug	27	16	49	8	0.00	0.08

[a]gl = glass; ol = olivine; pl = plagioclase; aug = augite.
[b]Phase proportions (wt%) estimated from least-squares linear regressions using the analytical data in Tables 4–7. All oxides were weighted by 1.00, except SiO_2 and Al_2O_3, which were weighted 0.40 and 0.50, respectively. The Na_2O and FeO losses are based on the results of the mass balance calculations and the original sample composition (Table 1). Most calculated losses are insignificant, except for FeO, runs 216–220.

Table 3. Precision of microprobe analyses, Juan de Fuca ridge basalt glass VG-2.

	1	S.D.	2
SiO_2	50.34	0.15	50.81
TiO_2	1.85	0.03	1.85
Al_2O_3	14.03	0.18	14.06
FeO	11.66	0.07	11.84
MnO	0.21	0.01	0.22
MgO	6.81	0.10	6.71
CaO	11.25	0.18	11.12
Na_2O	2.59	0.07	2.62
K_2O	0.20	0.01	0.19
P_2O_5	0.23	0.02	0.20
Total	98.85		99.49

1. Average and one standard deviation (S.D.) of 68 analyses.
2. Accepted analysis of VG-2 (Jarosewich et al., 1979).

and 0.06 for TiO_2, 0.05 and 0.46 for Al_2O_3, 0.04 and 0.44 for FeO, 0.01 and 0.04 for MnO, 0.05 and 0.38 for MgO, 0.05 and 0.3 for CaO, 0.04 and 0.10 for Na_2O, 0.01 and 0.03 for K_2O, and 0.01 and 0.03 for P_2O_5. The high values were found for the low-temperature experiments and result from the absence of perfect equilibrium, the fine grain size, and limitations of the analytical procedure. The lower range of these values is reasonably within or below the analytical

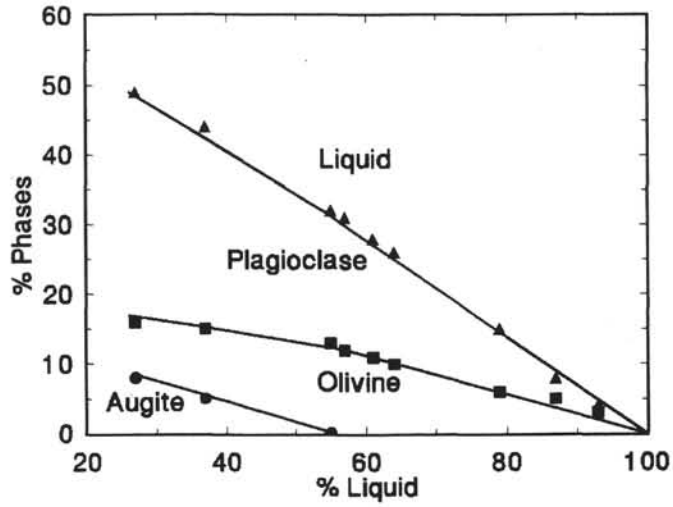

Figure 1. Experimental phase proportions vs. percentage of liquid. Phase proportions and % liquid have been estimated by least squares, linear regression, as described in the text.

precision of the electron microprobe analyses (Table 3). Elemental losses during the experiments were evaluated by mass-balancing the compositions of the constituting phases and comparing with the original composition (Table 1). The calculated Fe loss to the Pt wire is 3%–6% of the FeO of the original sample (Table 2), but may be below the significance for low-temperature experiments. The Na_2O losses are below significance for all experiments.

MINERAL-LIQUID EQUILIBRIA

In the experimental glasses, FeO, TiO_2, K_2O, and P_2O_5 all increase, while Al_2O_3 decreases with decreasing MgO (Table 4; Fig. 3). SiO_2, Na_2O, and CaO show relatively little variations, except for a slight decrease in CaO after the start of augite crystallization. These variations reflect a marked Fe-enrichment trend on the AFM diagram (Fig. 4). The Fe of the glasses has been redistributed between Fe_2O_3 and FeO, according to the algorithm proposed by Kilinc et al. (1983) and the FMQ oxygen buffer. These calculated Fe_2O_3 and FeO values, if not otherwise stated, are used throughout this paper.

Equilibrium olivine ranges in composition from Fo_{90} to Fo_{78} (Table 5), showing correlation with temperature (Fig. 5). The K_D values for the Fe^{2+} and Mg distribution between olivine and liquid (Fig. 6) ($K_D Fe/Mg$ (ol/liq) = $[X^{FeO}$ (ol) X^{MgO} (liq)]/$[X^{MgO}$ (ol) X^{FeO} (liq)]) average 0.31 (range, 0.29–0.32).

Equilibrium plagioclase ranges in composition from An_{79} to An_{67} (Table 6) and shows a dependence on temperature (Fig. 7A). Non-equilibrium plagioclase grains are present in most of the experiments, and are reflected in the compositional variation of individual microprobe analyses and the scatter observed in Figure 7. The $K_D Na/Ca$ (pl/liq) = $[X^{Na_2O}$ *(pl)* X^{CaO} (liq)]/$[X^{CaO}$ (pl)X^{Na_2O} (liq)] ranges between 0.55 and 0.99 and is strongly dependent on crystallization temperatures (Fig. 7B). The compositions of coexisting olivine and plagioclase show a systematic covariance (Fig. 8).

The Ti content of equilibrium augite is negatively correlated with Mg/(Mg + Fe), while Cr is positively correlated (Fig. 9). Total Al content (and Al^{iv} and Al^{vi}) shows little correlation with Mg/(Mg + Fe), and the Ti/Al ratios are systematically low (1/2-1/5), reflecting the relatively low TiO_2 content of the glasses. The Fe^{3+} content of the augites, estimated from balancing charge deficiencies vs. charge excesses (Papike et al., 1974), suggests the systematic presence of Fe^{3+} in the augites. However, the amount is uncertain because of the relatively few augites analyzed. Because of this, evaluation of the Fe^{2+}

Table 4. Chemical composition of experimental glasses.

	Run 237(4)[a]		Run 215(9)		Run 216(10)		Run 217(6)		Run 218(6)	
SiO_2	49.04	0.16	50.11	0.22	51.07	0.18	51.46	0.18	50.42	0.61
TiO_2	0.99	0.02	1.02	0.03	1.21	0.04	1.36	0.04	1.45	0.04
Al_2O_3	18.63	0.08	18.19	0.52	17.73	0.46	16.82	0.41	16.15	0.13
FeO^*	7.45	0.09	7.51	0.15	7.51	0.13	7.84	0.14	9.35	0.08
MnO	0.11	0.02	0.15	0.03	0.14	0.03	0.18	0.02	0.18	0.01
MgO	9.61	0.05	8.95	0.38	8.53	0.21	8.64	0.05	7.91	0.03
CaO	11.20	0.03	11.32	0.08	11.43	0.09	11.23	0.07	11.15	0.11
Na_2O	2.57	0.04	2.80	0.06	2.98	0.06	3.05	0.05	3.06	0.06
K_2O	0.08	0.01	0.08	0.01	0.09	0.01	0.10	0.01	0.11	0.01
P_2O_5	0.10	0.01	0.14	0.02	0.14	0.01	0.15	0.02	0.17	0.01
Cr_2O_3	0.05	0.02	0.03	0.01	0.05	0.01	0.05	0.01	0.05	0.02
Total	99.83		100.30		100.88		100.88		100.00	
$Mg/(Mg + Fe^{2+})$	0.724		0.709		0.699		0.693		0.635	
	Run 219(4)		Run 220(5)		Run 221(5)		Run 222(5)		Run 223(4)	
SiO_2	51.71	0.16	51.36	0.72	51.46	0.25	50.65	0.14	50.59	0.12
TiO_2	1.68	0.06	1.97	0.03	1.98	0.04	2.58	0.04	3.04	0.06
Al_2O_3	15.85	0.51	14.99	0.52	14.45	0.05	13.72	0.02	13.47	0.25
FeO^*	9.27	0.19	8.92	0.44	9.31	0.17	10.95	0.05	11.78	0.08
MnO	0.19	0.03	0.17	0.04	0.17	0.01	0.19	0.03	0.16	0.02
MgO	7.93	0.21	7.18	0.19	7.16	0.06	6.61	0.07	6.27	0.16
CaO	11.47	0.14	11.69	0.20	11.52	0.06	11.17	0.06	10.83	0.11
Na_2O	3.16	0.05	2.97	0.10	3.00	0.06	2.93	0.03	3.02	0.08
K_2O	0.12	0.01	0.14	0.01	0.15	0.02	0.18	0.03	0.19	0.01
P_2O_5	0.18	0.02	0.20	0.03	0.21	0.01	0.24	0.02	0.32	0.02
Cr_2O_3	0.06	0.04	0.04	0.00	0.04	0.01	0.04	0.02	0.02	0.02
Total	101.62		99.63		99.45		99.26		99.69	
$Mg/(Mg + Fe^{2+})$	0.638		0.641		0.614		0.556		0.525	

[a] Number in parenthesis refer to total number of analyses used for calculating each average (first column) and one standard deviation (second column).
FeO^* = all Fe as FeO. $Mg/(Mg + Fe^{2+})$ is calculated according to Kilinc et al. (1983) and the experimental conditions.

and Mg distribution assumes that all Fe occurs as Fe^{2+} for both liquid and augite. The K_DFe/Mg (cpx/liq) values (defined in a similar manner as for olivine) average 0.24 (Fig. 10).

EXPERIMENTAL LIQUID LINE OF DESCENT

The experimental glasses and augites have been projected into the normative basalt tetrahedron of Yoder and Tilley (1962), reducing the multicomponent system to the components plagioclase (pl), olivine (ol), diopside (di), and quartz (q) by using a CIPW molecular norm and by following the procedure outlined by Presnall et al. (1979). Iron has been distributed between Fe^{2+} and Fe^{3+}, according to Kilinc et al. (1983), and assumes the FMQ oxygen buffer. For augite, this assumption of the redox state of Fe is an approximation in the absence of better estimates.

Figure 11 depicts a perspective drawing of the pseudoquaternary system pl-di-ol-q, and Figure 12 presents two pseudoternary projections ol-di-q and ol-pl-q. As expected, initially the liquid compositions move away from a point on the line pl-ol, reflecting the proportions of the crystallizing phases. The starting composition is hypersthene-normative. After augite begins to crystallize, the liquids are quartz-normative and move away from a point on the plane pl-ol-di in accordance with the equilibrium phase assemblage.

The relative proportions of the crystallizing mineral phases for the multisaturated liquids reaches 22 wt% olivine, 67% plagioclase, and 11% augite. These proportions are significantly more felsic than commonly observed experimentally for transitional and tholeiitic basalts of the ocean floor, which typically average 29% olivine, 53% plagioclase, and 18% augite (Thy, 1991; Grove and Bryan, 1983; Tormey et al., 1987). Mildly alkalic basalts will crystallize an even more mafic assemblage (Mahood and Baker, 1986; Thy et al., 1991).

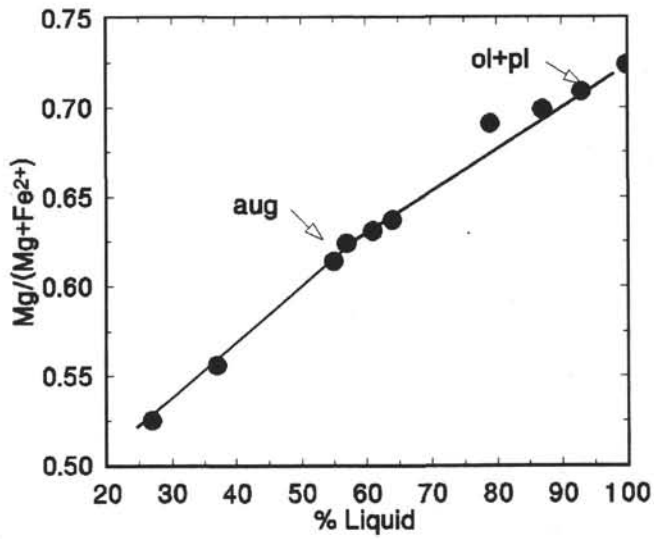

Figure 2. $Mg/(Mg + Fe^{2+})$ of the experimental glasses vs. percentage of liquid remaining. Fe^{2+}/Fe^{3+} was calculated according to Kilinc et al. (1983). The appearance of liquidus phases is indicated; ol = olivine; pl = plagioclase; aug = augite.

DISCUSSION

Experimental equilibrium is suggested by the exchange of Fe and Mg between olivine or augite and coexisting liquid. The obtained K_D for olivine and liquid (0.31) is consistent with that commonly observed (Roeder and Emslie, 1970; Mahood and Baker, 1986; Baker and Eggler,

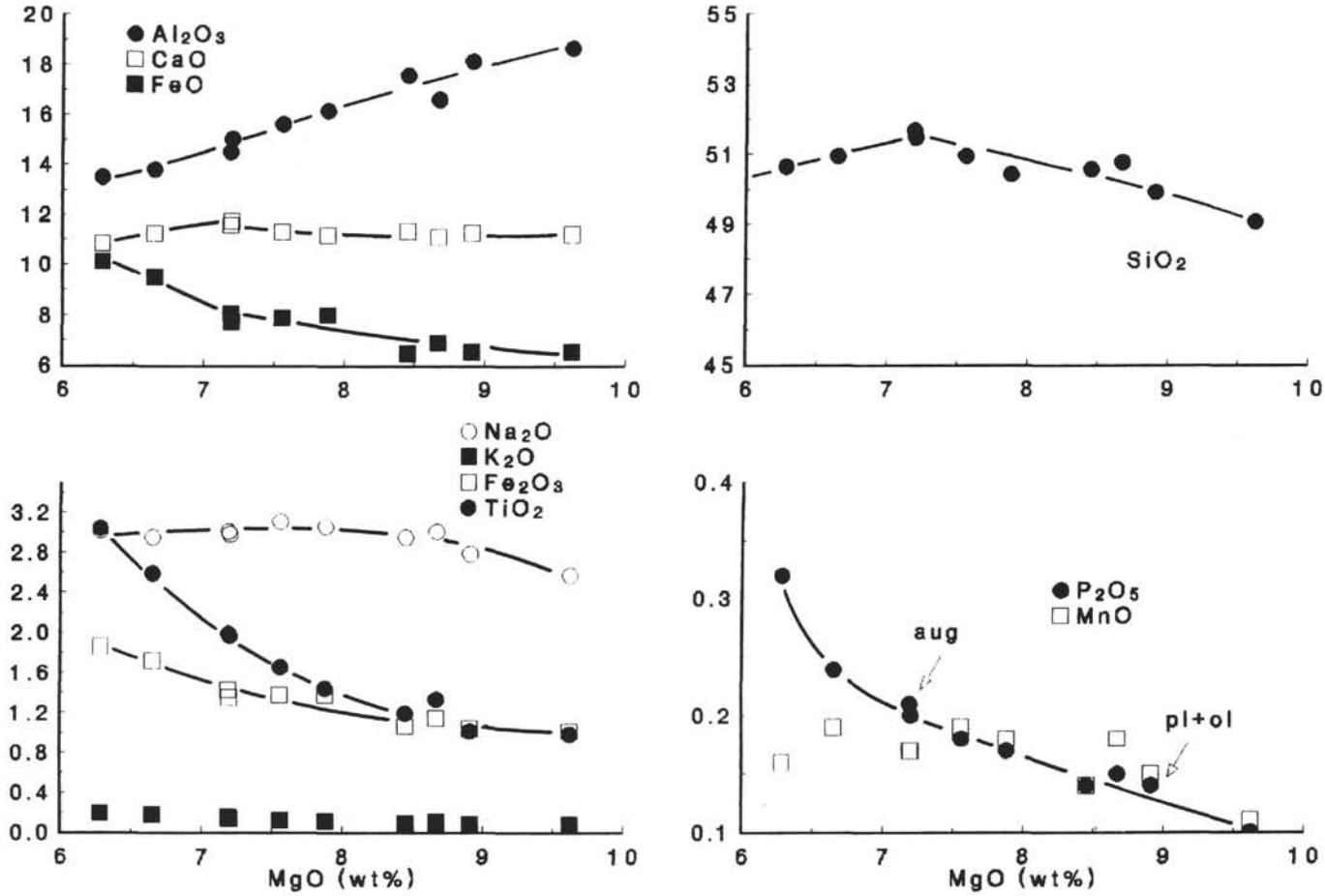

Figure 3. Composition of the experimental glasses plotted vs. MgO (wt%). Oxides calculated to 100% with Fe distributed between FeO and Fe_2O_3 after Kilinc et al. (1983), assuming the FMQ oxygen buffer. The start of crystallization of augite (aug) and plagioclase and olivine (pl + ol) is indicated.

1987; Ulmer, 1989; Ussler and Glazner, 1989) and is independent of temperature. This contrasts with the observation of Bender et al. (1978) that K_D varies as a function of temperature or degree of crystallization. The K_D for augite and liquid found here is 0.24, which appears to be independent of temperature. This finding is consistent with the experimental observations of Grove and Bryan (1983) and Thy et al. (1991) and for natural lavas by Perfit and Fornari (1983).

The exchange coefficients for Na and Ca between plagioclase and liquid are strongly dependent on crystallization temperature and degree of crystallization. The K_D values range from 0.60 at 1230°–1220°C to 0.99 at about 1150°C. A quantitatively similar temperature dependence was observed by Ussler and Glazner (1989). Modeling crystal fractionation without taking into consideration the temperature dependence of K_D will lead to relatively higher Na contents of residual liquids. Another complicating effect is that K_D for plagioclase and liquid will be dependent on composition (Drake, 1976; Glazner, 1984; Ussler and Glazner, 1989).

The augites are hypersthene-normative (Fig. 12). This places the thermal divide defined by coexisting augite, olivine, and plagioclase within the hypersthene-normative volume and constrains the possible liquid evolution path toward increasing normative quartz (Fig. 12). The location of the multisaturated liquids is consistent with the liquid line of descent defined by similar experiments on tholeiitic basalts by Walker et al. (1979) and Grove and Bryan (1983), among many others. Because the starting composition is hypersthene-normative (Fig. 12), the liquid path during equilibrium crystallization can be predicted to reach low-Ca pyroxene-saturated, pseudoinvariant relations and there to be fully consumed. However, because of the relatively low, but unknown, amount of liquid remaining at this point, direct determination was not possible. Also, the effect of a possible low-temperature crystallization of Fe-Ti oxide minerals was not determined. The liquid line of descent, nevertheless, is typical for olivine tholeiitic basalts.

The similarities between the produced crystallization order (plagioclase, olivine; augite) with that petrographically observed (plagioclase; olivine; augite; titanomagnetite) suggest that the Hole 797C sills crystallized at relatively low-pressure and at a low water activity. The strong FeO and TiO_2-enrichment and Al_2O_3-depletion experimentally observed for the Hole 797C basalt is typical for tholeiitic evolution trends and is an effect of the dominance of plagioclase in the crystallizing assemblage. The low-temperature experimental liquids are ferrobasalts that are similar to those seen at slow-spreading segments of active rift zones. In this respect, the experimental liquids show some general similarities with the Fe- and Ti-enriched basalts drilled in the lower part of Hole 797C (Tamaki et al., 1990). On the other hand, it is clear that the evolved high-Al basalts of Hole 794C cannot be produced by low-pressure, anhydrous crystallization. Instead, these compositions are more likely to have evolved during crystallization under high pressure or high water activity, either of which can suppress plagioclase crystallization and consequently produce Al_2O_3 enrichments (Grove and Baker, 1984; Michael and Chase, 1987). The experiments, therefore, have no direct bearing on the origin of the high-Al basalts.

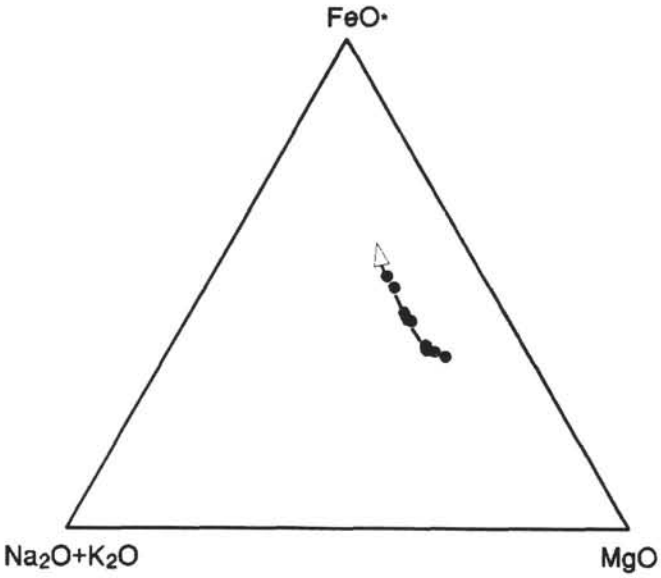

Figure 4. AMF (Na_2O + K_2O, FeO^*, MgO) diagram for the experimental glasses. Fe is calculated as total FeO (FeO^*). Arrow indicates direction of falling temperature.

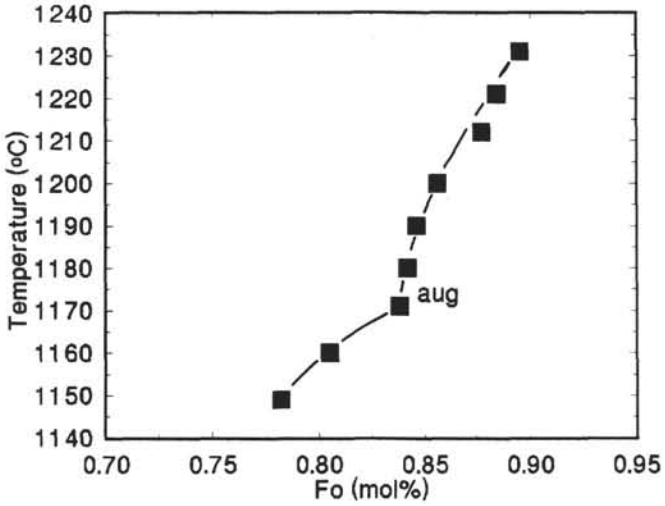

Figure 5. Crystallization temperature (°C) vs. Fo mol% for olivine. The bend in the liquidus slope coincides with the appearance of augite (aug).

CONCLUSIONS

One-atmosphere, anhydrous melting experiments performed on a primitive basalt from the upper part of Hole 797C produced residual liquids, which show a typical tholeiitic evolution trend with increasing FeO and TiO_2 as a function of decreasing temperature and increasing degree of crystallization. The similarities between the experimental crystallization order and that observed in the sills support the conclusion that the sills crystallized at very low-pressures and low water activities. From a major-element point of view, the experimental data can explain the Fe- and Ti-enriched sills of the lower part of Hole 797C, but have no direct bearing on the origin of the relatively evolved high-Al basalts of Hole 794C.

ACKNOWLEDGMENTS

Part of this work was done in G.E. Lofgren's experimental petrology laboratory at NASA's Johnson Space Center. S.R. Yang helped with the microprobe and A.B. Lanier and W. Carter with the experimental procedures and equipment. S. Grundvig, J. Allan, and S. Yamashita helped with obtaining reliable XRF analyses of the starting material. The Danish Natural Science Research Council supported the author during Leg 127. The shore-based study was initiated during a U.S. National Research CouncilNASA Research Associateship. Critical comments from J. Allan, M. Fisk, and an anonymous reviewer improved the manuscript.

REFERENCES

Baker, D. R., and Eggler, D. H., 1987. Compositions of anhydrous and hydrous melts coexisting with plagioclase, augite, and olivine or low Ca pyroxene from 1 atm to 8 kbar: application to the Aleutian volcanic center of Atka. *Am. Mineral.,* 72:12–28.

Bender, J. F., Hodges, F. N., and Bence, A. E., 1978. Petrogenesis of basalts from the project FAMOUS area: experimental study from 0 to 15 kbars. *Earth Planet. Sci. Lett.,* 41:277–302.

Donaldson, C. H., Williams, R. J., and Lofgren, G., 1975. A sample holding technique for study of crystal growth in silicate melts. *Am. Mineral.,* 60:324–326.

Drake, M. J., 1976. Plagioclase-melt equilibria. *Geochim. Cosmochim. Acta,* 40:457–465.

Glazner, A. F., 1984. Activities of olivine and plagioclase components in silicate melts and their application to geothermometry. *Contrib. Mineral. Petrol.,* 88:260–268.

Grove, T. L., and Baker, M. B., 1984. Phase equilibrium controls on the tholeiitic versus calc-alkaline differentiation trends. *J. Geophys. Res.,* 89:3253–3274.

Grove, T. L., and Bryan, W. B., 1983. Fractionation of pyroxene-phyric MORB at low pressure: an experimental study. *Contrib. Mineral. Petrol.,* 84:293–309.

Jarosewich, E., Parkes, A. S., and Wiggins, L. B., 1979. Microprobe analyses of four natural glasses and one mineral: an interlaboratory study of precision and accuracy. *Smithsonian Contrib. Earth Sci.,* 22:53–67.

Kilinc, A., Carmichael, I.S.E., Rivers, M. L., and Sack, R. O., 1983. The ferric-ferrous ratio of natural silicate liquids equilibrated in air. *Contrib. Mineral. Petrol.,* 83:136–140.

Lofgren, G. E., 1983. Effect of heterogeneous nucleation on basaltic textures: a dynamic crystallization study. *J. Petrol.,* 24:229–255.

Mahood, G. A., and Baker, D. R., 1986. Experimental constraints on depth of fractionation of mildly alkalic basalts and associated felsic rocks: Pantelleria, Strait of Sicily. *Contrib. Mineral. Petrol.,* 93:251–264.

Michael, P. J., and Chase, R. L., 1987. The influence of primary magma composition, H_2O and pressure on mid-ocean ridge basalt differentiation. *Contrib. Mineral. Petrol.,* 96:245–263.

Papike, J. J., Cameron, K. L., and Baldwin, K., 1974. Amphiboles and pyroxenes: characterization of other than quadrilateral components and estimates of ferric iron from microprobe data. *Geol. Soc. Am. Abstr. Programs,* 6:1053–1054. (Abstract)

Perfit, M. R., and Fornari, D. J., 1983. Geochemical studies of abyssal lavas recovered by DSRV Alvin from eastern Galapagos rift, Inca transform, and Ecuador rift. 2. Phase chemistry and crystallization history. *J. Geophys. Res.,* 88:10530–10550.

Presnall, D. C., Dixon, J. R., O'Donnell, T. H., and Dixon, S. A., 1979. Generation of mid-ocean tholeiites. *J. Petrol.,* 20:3–35.

Roeder, P. L., and Emslie, R. F., 1970. Olivine-liquid equilibria. *Contrib. Mineral. Petrol.,* 29:275–289.

Tamaki, K., Pisciotto, K., Allan, J., et al., 1990. *Proc. ODP, Init. Repts,* 127: College Station, TX (Ocean Drilling Program).

Thy, P., 1991. High and low pressure phase equilibria of a mildly alkalic lava from the 1965 Surtsey eruption: experimental results. *Lithos,* 26:223–243.

Thy, P., Lofgren, G. E., and Imsland, P., 1991. Melting relations and the evolution of the Jan Mayen magma system. *J. Petrol.,* 32:303–332.

Tormey, D. R., Grove, T. L., and Bryan, W. B., 1987. Experimental petrology of normal MORB near the Kane fracture zone: 22°–25°N, mid-Atlantic ridge. *Contrib. Mineral. Petrol.,* 96:121–139.

Ulmer, P., 1989. The dependence of the Fe^{2+}-Mg cations-partitioning between olivine and basaltic liquid on pressure, temperature and composition. An experimental study to 30 kbars. *Contrib. Mineral. Petrol.,* 101:261–273.

Ussler, W., and Glazner, A. F., 1989. Phase equilibria along a basalt-rhyolite mixing line: implications for the origin of calc-alkaline intermediate magmas. *Contrib. Mineral. Petrol.*, 101:232–244.

Walker, D., Shibata, T., and DeLong, S. E., 1979. Abyssal tholeiites from the Oceanographer fracture zone. II. Phase equilibria and mixing. *Contrib. Mineral. Petrol.*, 70:111–125.

Williams, R. J., and Mullins, O., 1981. JSC systems using solid ceramic oxygen electrolyte cells to measure oxygen fugacities in gas-mixing systems. *NASA Tech. Mem.*, 58234.

Yoder, H. S., and Tilley, C. E., 1962. Origin of basalt magmas: an experimental study of natural and synthetic rock systems. *J. Petrol.*, 3:342–532.

Date of initial receipt: 27 November 1990
Date of acceptance: 15 November 1991
Ms 127/128B-203

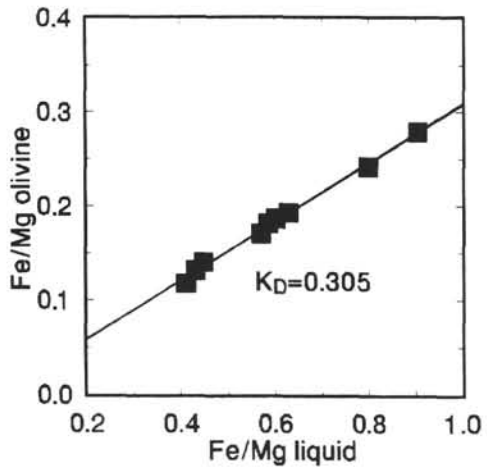

Figure 6. Fe/Mg for olivine vs. Fe/Mg for coexisting liquid calculated, as described in text. K_D is estimated from the slope of the linear regression to 0.305.

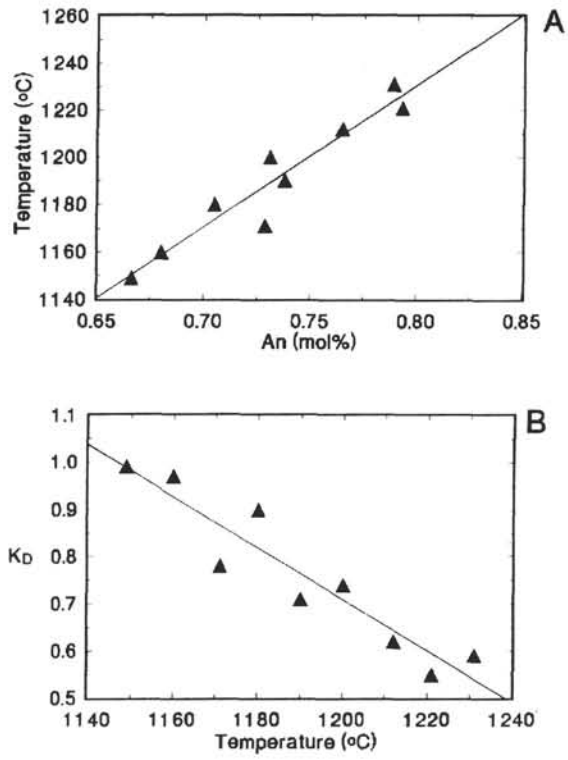

Figure 7. A. Crystallization temperature (°C) vs. An mol% for plagioclase. **B.** $K_D^{Na/Ca}$ (pl/liq) vs. crystallization temperature (°C) for the experimental plagioclases.

Table 5. Chemical composition of experimental olivine.

	Run 215(6)a		Run 216(6)		Run 217(4)		Run 218(4)		Run 219(3)	
SiO_2	41.67	0.35	41.16	0.27	40.05	0.47	39.44	0.19	39.23	0.10
FeO	10.38	0.52	11.39	0.33	11.86	0.10	14.04	0.05	14.47	0.17
MnO	0.17	0.02	0.22	0.02	0.20	0.02	0.24	0.02	0.26	0.02
MgO	49.55	1.01	48.52	0.46	47.44	0.50	46.16	0.66	44.66	0.13
CaO	0.29	0.02	0.40	0.03	0.43	0.03	0.49	0.08	0.45	0.01
Total	102.06		101.69		99.98		100.37		99.07	
Fo mol%	89.5		88.4		87.7		85.4		84.6	
[b]K_D	0.29		0.31		0.32		0.30		0.31	

	Run 220(4)		Run 221(4)		Run 222(5)		Run 223(3)	
SiO_2	39.41	0.23	39.65	0.20	39.06	0.34	38.98	0.16
FeO	14.74	0.20	15.42	0.08	18.08	0.15	20.19	0.12
MnO	0.32	0.05	0.25	0.02	0.29	0.03	0.26	0.03
MgO	44.22	0.51	44.77	0.17	41.91	0.78	40.55	0.42
CaO	0.51	0.06	0.49	0.06	0.49	0.06	0.46	0.02
Total	99.20		100.58		99.83		100.44	
Fo mol%	84.2		83.8		80.5		78.2	
[b]K_D	0.31		0.31		0.30		0.31	

[a]Number in parenthesis refers to total number of analyses used for calculating each average (first column) and one standard deviation (second column).
[b]K_D for the distribution of Fe and Mg between olivine and liquid calculated assuming the FMQ oxygen buffer and Fe^{2+}/Fe^{3+} according to Kilinc et al. (1983) (see text).

Table 6. Chemical composition of experimental plagioclase.

	Run 215(5)[a]		Run 216(5)		Run 217(6)		Run 218(4)		Run 219(5)	
SiO_2	50.15	0.47	49.68	0.31	49.24	1.16	50.05	1.05	50.27	0.44
TiO_2	0.02	0.01	0.04	0.02	0.04	0.01	0.05	0.02	0.06	0.02
Al_2O_3	32.30	1.45	32.04	0.56	31.94	1.19	31.63	0.43	31.84	0.78
FeO	0.60	0.05	0.69	0.10	0.62	0.09	0.67	0.04	0.74	0.13
MgO	0.28	0.06	0.25	0.05	0.34	0.09	0.27	0.03	0.32	0.11
CaO	16.31	0.36	16.42	0.24	15.59	0.84	14.91	0.67	15.10	0.28
Na_2O	2.40	0.19	2.35	0.12	2.63	0.46	3.01	0.31	2.95	0.18
K_2O	0.02	0.01	0.02	0.01	0.02	0.01	0.03	0.01	0.02	0.01
Total	102.08		101.49		100.42		100.62		101.30	
An mol%	0.789		0.793		0.765		0.731		0.738	
^bK_D	0.59		0.55		0.62		0.74		0.71	

	Run 220(5)		Run 221(8)		Run 222(4)		Run 223(5)	
SiO_2	50.94	1.07	50.77	0.74	52.23	1.10	52.58	1.20
TiO_2	0.07	0.02	0.05	0.01	0.05	0.01	0.06	0.02
Al_2O_3	30.41	1.36	31.97	0.61	30.38	0.73	30.34	0.62
FeO	0.71	0.12	0.61	0.06	0.73	0.06	0.79	0.09
MgO	0.26	0.08	0.20	0.03	0.25	0.09	0.19	0.02
CaO	14.33	0.79	14.85	0.50	13.67	0.71	13.37	0.85
Na_2O	3.29	0.39	3.03	0.29	3.52	0.37	3.69	0.38
K_2O	0.04	0.01	0.03	0.01	0.05	0.01	0.03	0.01
Total	100.05		101.51		100.88		101.05	
An mol%	0.705		0.729		0.680		0.666	
^bK_D	0.90		0.78		0.97		0.99	

[a]Number in parenthesis refers to total number of analyses used for calculating each average (first column) and one standard deviation (second column).
[b]K_D for the distribution of Na and Ca between plagioclase and liquid (see text).

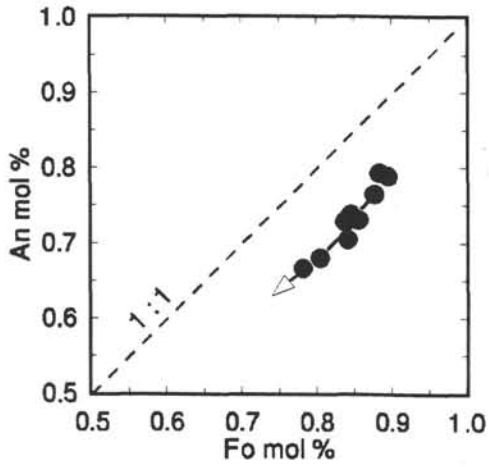

Figure 8. An mol% of equilibrium plagioclase vs. Fo mol% for coexisting olivine. Arrow indicates direction of falling temperature.

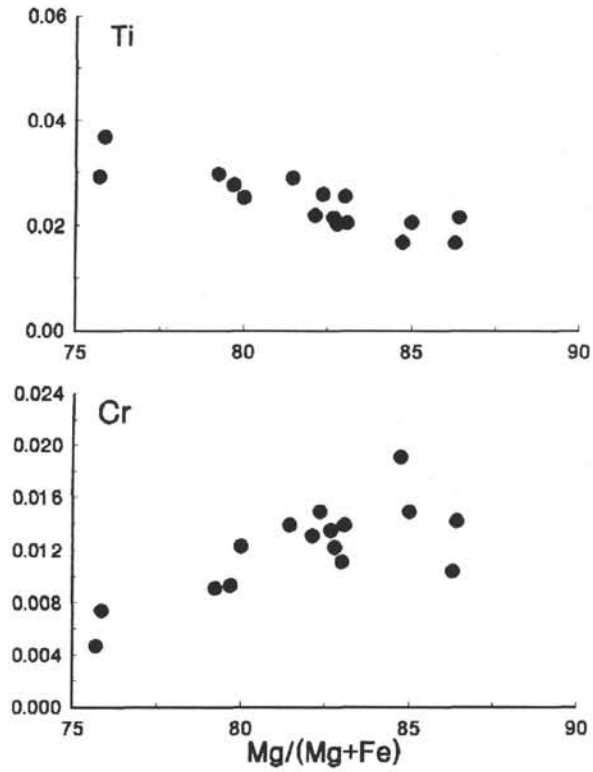

Figure 9. Minor elements Cr and Ti (calculated to 6 oxygens) vs. Mg/(Mg + Fe) of augite. All analyses are shown, and all Fe was assumed to occur as FeO. A few analyses plotting with Mg/(Mg + Fe) above 0.85 are considered disequilibrium phases.

Table 7. Chemical composition of experimental augite.

	Run 221(4)[a]		Run 222(4)		Run 223(5)	
SiO_2	52.66	0.44	52.24	0.48	51.48	0.70
TiO_2	0.74	0.16	0.79	0.08	1.07	0.15
Al_2O_3	2.30	0.69	2.33	0.16	2.56	0.52
FeO*	5.32	0.49	6.46	0.53	7.51	0.97
MnO	0.15	0.02	0.16	0.01	0.17	0.02
MgO	16.91	0.97	16.64	0.34	16.07	1.31
CaO	20.05	0.78	20.47	0.32	20.46	0.66
Na_2O	0.30	0.01	0.28	0.02	0.36	0.03
Cr_2O_3	0.51	0.12	0.45	0.03	0.31	0.12
Total	98.94		99.82		99.99	
En (mol%)	49.3		47.6		45.9	
Fs (mol%)	8.7		10.4		12.0	
Wo (mol%)	42.0		42.0		42.1	
[b]K_D	0.24		0.24		0.25	

[a]Number in parenthesis refers to total number of analyses used for calculating each average (first column) and one standard deviation (second column).
[b]K_D for the distribution of Fe and Mg between augite and liquid calculated assuming all iron as FeO (see text).

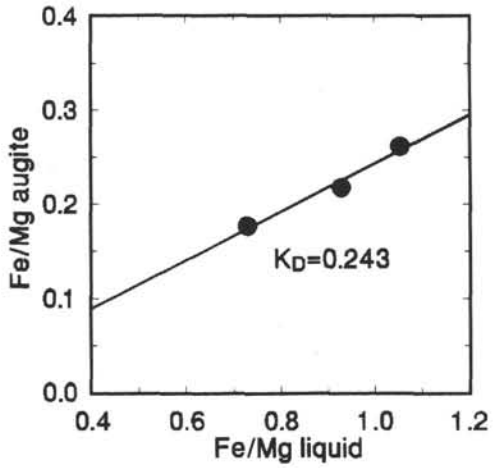

Figure 10. Fe/Mg for augite vs. Fe/Mg for coexisting liquid, calculated as described in text. K_D is estimated from the slope of the linear regression to 0.243.

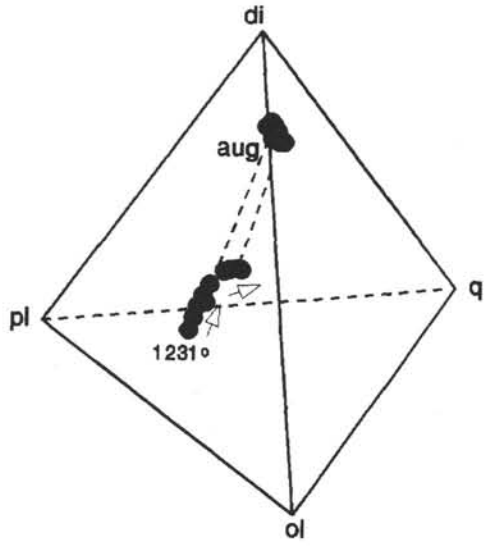

Figure 11. Pseudoquaternary normative projection of experimental liquids and augites. Molecular CIPW-norm calculation and projection methods are those of Presnall et al. (1979), except that Fe was distributed between FeO and Fe_2O_3, according to Kilinc et al. (1983). The range in tie-lines between coexisting augite and liquid is indicated. The temperature 1231° is the first appearance of olivine and plagioclase. Arrows indicate falling temperature.

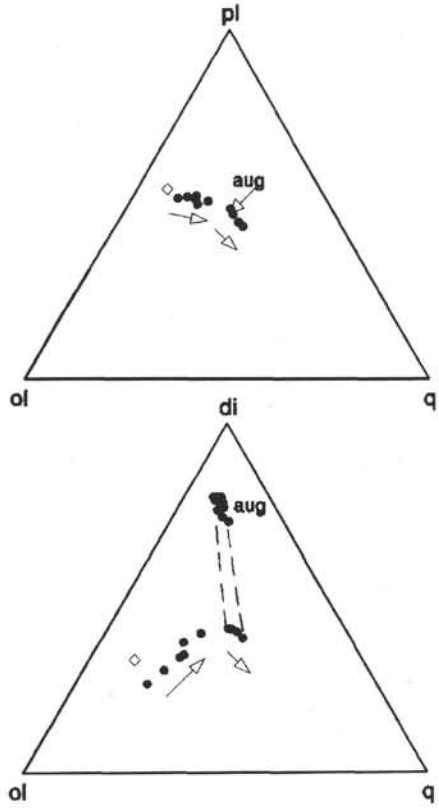

Figure 12. Pseudoternary normative projections of experimental liquids and augites. Data, calculations, and projection methods as for Figure 11. The range in tie-lines between coexisting augite and liquid is indicated on the ol-di-q projection, while the income of augite is indicated for the ol-pl-q projection. Arrows indicate direction of falling temperature. ol = olivine; pl = plagioclase; di = diopside; q = quartz; aug = augite. Open diamond is the starting composition (Table 1).